**20th WCNDT** 20th World Conference on Non-Destructive Testing

Songdo Convensia, Incheon, Korea, 27~31 May 2024

**NDT**net

**eJNDT**

# The Dispersion Calculator - A Free Software for Calculating Dispersion Curves of Guided Waves

## A. HUBER[1]

[1] German Aerospace Center (DLR), Augsburg, Germany
Contact: armin.huber@dlr.de

**Abstract**

The nondestructive inspection of components by means of guided waves is an emerging technology in fields like aerospace or pipeline construction and maintenance. The guided waves' capability of propagating many meters in a structure is utilized for swift inspection tasks as well as structural health monitoring. The German Aerospace Center uses Lamb waves for the quality assurance of large-scale aerospace vehicle components made from carbon composites. However, the use of guided waves in NDT requires knowledge of the dispersion curves. DISPERSE is the most renown software for the calculation of dispersion curves. This paper presents the open source Dispersion Calculator (DC). The MATLAB®-based DC is an interactive and fully validated software for the computation of dispersion curves and mode shapes of guided waves in isotropic plates and multilayered anisotropic composites. Damping caused by viscoelasticity and fluid-loading can be considered. DC features the capability of calculating laminates consisting of several hundreds of layers so that even the largest specimens, like rocket booster pressure vessels, can be calculated. This is made possible through the implementation of the stiffness matrix method. DC is also able to distinguish the different mode families, like symmetric, antisymmetric, and nonsymmetric Lamb, shear horizontal, and Scholte waves, depending on the symmetry and coupling properties of a given layup. Lastly, DC features a highly efficient and robust dispersion curve tracing algorithm. DC is available at GitHub, and it has gained many users world-wide since its initial release in 2018.

Keywords: Guided waves, Dispersion, Numerical modeling, Stiffness matrix method, Software, Composites

## 1. Introduction

A high demand for carbon fiber reinforced polymers (CFRP) is evident in the manufacturing of high-performance components such as aircraft fuselages or rocket booster pressure vessels. The superior strength-to-weight ratio of CFRP compared to traditional steel or aluminum alloys allows the vehicles to operate more efficiently. Disadvantages of CFRP are the high cost of the raw material and the sophisticated production processes. It is therefore convenient to use nondestructive inspection methods (NDI) such as ultrasonic testing (UT) on such valuable components. As two-sided access to the component is often impossible, like in the case of pressure vessels or pipes, and because the inspection should go as fast as possible, guided waves offer a great opportunity to fulfil theses basic requirements.

The first description of flaw detection in sheets and tubes immersed in water by means of Rayleigh and Lamb waves was presented by Viktorov in 1967 [1]. Luukkala *et al.* proposed a contactless test method for paper and metal plates based on Lamb waves [2], [3]. Many applications have been established since then, and with the advent of composite materials in automotive and aerospace industries in the early 1990s, the nondestructive testing and evaluation processes have gained significant complexity. The ability of guided waves to propagate many meters in a waveguide is utilized for pipe inspection [4], [5]. Another application is the inspection of bonding [6], [7]. Other relevant studies on NDI and structural health monitoring (SHM) on composite structures are given in Refs. [8]-[15]. The noncontact method of air-coupled ultrasonic testing (ACUT) by means of Lamb waves is particularly useful

in cases where a liquid coupling medium might inflict damage to the component to be inspected or if the inspection method shall be integrated as an inline quality assurance method, as the case at the German Aerospace Center (DLR) [16]. Castaings *et al.* have done significant work on the single-sided air-coupled ultrasonic testing of composites by means of Lamb waves [17]-[20], whereas Solodov *et al.* have utilized them for transmissive inspection [21]-[23]. Mechanically induced fatigue on composites has been monitored by means of Lamb waves by Rheinfurth and Schmidt *et al.* [24], [25].

However, unlike bulk waves utilized in conventional UT-methods like in the normal transmission mode or in the pulse-echo mode, guided waves are dispersive, which means that their phase and group/energy velocities are frequency-dependent. It is therefore essential to have the specific dispersion diagram at hand to be able to perform an inspection at all. Such diagrams can be calculated, but the programming is a difficult task, in particular if one is interested in multilayered anisotropic composites. DISPERSE [26], [27] (Imperial College London, London, UK) is the most renown software for the calculation of dispersion curves. It has been developed since the early 1990s by Lowe and Pavlakovic, and with its versatility and speed of computation, it sets a high standard for any software to come up. However, DISPERSE cannot model laminates consisting of more than 60 layers, whereas modern rocket booster pressure vessels can have up to 360 layers in some areas. As the layups can be quite complicated, no grouping of layers is possible to reduce the computational expense. As no other software was available that could solve the problem, the author started in 2016 to develop the Dispersion Calculator (DC) in MATLAB® (The MathWorks®, Natick, MA, USA). DC version 1.0 was released in 2018, and many more advanced versions have been released since then. DC can be downloaded on GitHub [28] as a stand-alone software as well as the MATLAB® code. However, there are several free softwares for calculating guided wave dispersion diagrams. GUIGUW [29], [30] is a software package developed and released by Marzani and Bocchini in 2011. As it is based on the *semi-analytical finite-element* (SAFE) method, it is able to model waveguides of arbitrary cross sections. Another contender, the open source MATLAB® toolbox ElasticMatrix [31], [32], was released by Ramasawmy *et al*. in 2020. It is able to compute dispersion curves for multilayered plates made of isotropic and transversely isotropic layers where the wave propagation occurs in a material plane of symmetry. However, this covers decoupled polarization only, so far excluding the majority of composites where we have arbitrary fiber orientations and wave propagation directions. Next, the Dispersion Box [33], [34] was released by Orta *et al.* in 2022. Up to six different methods can be used simultaneously to compute dispersion diagrams for viscoelastic composites with arbitrary layer stackings and propagation directions. In the same year, Kiefer published GEW dispersion script for MATLAB® [35], which uses the *spectral collocation method* (SCM). Finally, as the third contender appearing in 2022, Liu *et al.* released SAFEDC [36]. This software has a similar layout as DC, but uses SAFE for the modeling of waveguides with arbitrary cross sections and general anisotropy. At the time of this paper, SAFEDC does not include damping, but its implementation is planned in the future, along with more features mentioned in a preprint cited on SourceForge [36].

To be able to calculate large numbers of layers, DC uses the *stiffness matrix method* (SMM), which belongs to the class of root-finding methods. SMM is a reformulation of the *transfer matrix method* (TMM) conducted by Rokhlin and Wang [37], [38]. SMM is also well-documented in the highly recommended book by Rokhlin *et al.* [39]. Another particularly useful source for the implementation of SMM is the paper of Kamal and Giurgiutiu [40]. TMM for a layered medium was developed by Thomson [41], and Haskell corrected a small error in

Thomson's work [42]. Nayfeh extended TMM to generally anisotropic multilayered media [43], [44]. Although employing TMM, Nayfeh's excellent book [45] served as the backbone for the programming of DC. However, TMM suffers from a numerical instability when the product of the layer thickness and frequency is large. Many attempts to overcome the problem failed subsequently. A different approach is the *global matrix method* (GMM), proposed by Knopoff [46]. Here, the equations of all layers are contained in a large single matrix. Schmidt and Tango showed that this method is numerically stable [47]. Mal [48] extended GMM to anisotropic multilayered media, and Kausel and Roesset [49] conducted a reformulation for isotropic cases. A well-organized and instructive discussion of TMM and GMM is provided by Lowe [50]. However, the drawback of GMM is that it becomes slow upon calculating many layers, owing to the large size of the global matrix. DISPERSE uses GMM, and this is the reason why, although very fast in general, it becomes cumbersome when several tens of layers are involved. The newer SMM is possibly the most powerful root-finding method for multilayered problems, in particular when there are several hundreds of layers. SMM is numerically unconditionally stable, and it retains the concise form and efficiency of TMM. Huber and Sause [51] and Huber [52], [53] implemented mode family specific dispersion equations into SMM to improve efficiency and robustness of the dispersion curve tracing. The authors demonstrated the separate tracing of symmetric, antisymmetric, and nonsymmetric Lamb and shear horizontal (SH) waves in composite layups containing up to 400 layers. The dispersion diagrams presented by Huber and Sause were obtained with DC.

The main disadvantage of root-finding methods is that they are limited to flat and cylindrical waveguides. An alternative is therefore the discretizing SAFE method, made popular by Gavric [54]. The SAFE method discretizes the waveguide's cross section into finite elements, allowing the modeling of guided waves in complex geometries. At the same time, the wave propagation direction is solved analytically, which makes this approach more efficient than the standard finite element method (FEM). The latest and possibly most powerful discretizing method is SCM, developed by Quintanilla *et al.* [55]. It is similar to the SAFE method in that it is using a one-dimensional mesh over the system's thickness, but SCM possesses a higher accuracy and speed of computation. Instead of solving a differential equation directly, SCM uses a spectral approximation, which satisfies the differential equation and boundary conditions. The paper claims that SCM is easier to code than root-finding methods, that it is faster, and, most importantly, that it does not miss any modal solution. In 2017, the same authors developed a classification of multilayered anisotropic waveguides according to their symmetry and coupling properties [56]. All crystal classes and independent axes configurations can be assigned to one of only five different categories. A crucial benefit is that modal solutions can be separated into mode families for which dispersion curves do not cross. This helps avoid the well-known jumping mode problem. Furthermore, one can save time by computing only a single mode family if one is not interested in the others. More recently, SCM was used also to model leaky waves [57], [58].

Another class of computation methods are the approximative *plate theories*. Basically, the displacement field versus the plate thickness is represented by polynomial functions of a certain order. The first *advanced plate theory* (APT), also called *first order shear deformation theory* (1-SDT) was presented by Mindlin [59] in 1951. This theory gives accurate results for the lowest antisymmetric modes, but fails to model any higher order modes. By raising the order of the polynomial, the approximation error decreases, and the number of modes that can be calculated increases, at the cost of computational efficiency. Higher order plate theories have been developed by Withney and Sun [60] (2-SDT, 5 symmetric and 3 antisymmetric modes),

by Wang and Yuan [61] (3-SDT, 5 symmetric and 6 antisymmetric modes), and an enhanced 3-SDT by Zhao *et al.* [62]. Recently, Orta *et al.* [63] introduced a 5-SDT for multilayered composite plates allowing the calculation of 9 symmetric and 9 antisymmetric modes at high efficiency (less than a second on a standard laptop).

As the main requisite imposed on DC was that it must be able to compute multilayered composites with several hundreds of layers, the author decided to employ SMM. And because DC should separate the various mode families, similar as it was demonstrated with SCM, the author implemented mode family-specific dispersion equations into SMM. The advantage of the discretizing methods that they can model waveguides with complex cross sections, whereas root-finding methods are limited to flat and cylindrical structures, does not help in the plate-like laminates commonly present in aerospace. Fortunately, the solutions obtained with SMM for flat structures are valid in good approximation for curved structures with a radius significantly larger than the guided waves' wavelength. This is often the case in aircraft fuselages or rocket booster pressure vessels. Alternatively, in most cases, there is one dimension for which the component is flat. Furthermore, SMM as a root-finding method allows to maintain the accuracy of the modal solutions throughout the dispersion diagram because bisections or Newton-Raphson's method are performed until the desired accuracy is reached. In discretizing methods, accuracy depends on the number of through-thickness samples. Because the mode shapes become more complex with increasing frequency and mode order, accuracy decreases. Multiple computations must be performed to see if the solutions converge. Using approximative methods like the higher order plate theories in DC is not an option because the accuracy depends on case-dependent shear correction factors. The user would always question the accuracy of results, therefore requiring a reference calculation with an exact method. Even if the approximative methods are very fast, it is considered more important that the solutions are within tolerance and that the user can trust them.

## 2. The Dispersion Calculator

DC is an interactive and fully validated open source software for the computation of dispersion curves and mode shapes of guided waves in flat isotropic plates and multilayered anisotropic laminates such as composites. The specimens can be surrounded with different inviscid fluids in the upper and lower half-spaces, leading to damping through energy leakage. The user can edit available or add and remove custom materials. Viscoelastic damping is introduced through complex engineering constants and stiffnesses. DC comes with a user's manual, which provides more detailed insight than this paper.

### 2.1 Overview

DC offers an easy-to-use graphical user interface (GUI) (see for example the "Anisotropic" tab in Fig. 1). Basically, it provides only the parameter setting interfaces like editable fields and buttons as well as some output windows displaying data and other information. All plots like dispersion diagrams or mode shapes are plotted in extra windows, which open when the user presses the corresponding button. This basic arrangement improves user-friendliness by avoiding options in multi-leveled sub menus where they are out of sight of the user initially. Instead, DC provides all options that are related to one task in just one tab. For example, in the

"Isotropic" tab, the user can set up the specimen, define the computational parameters, calculate the dispersion curves, through thickness profiles, mode shapes, adjust the plot layout, and manage the export of data and plots.
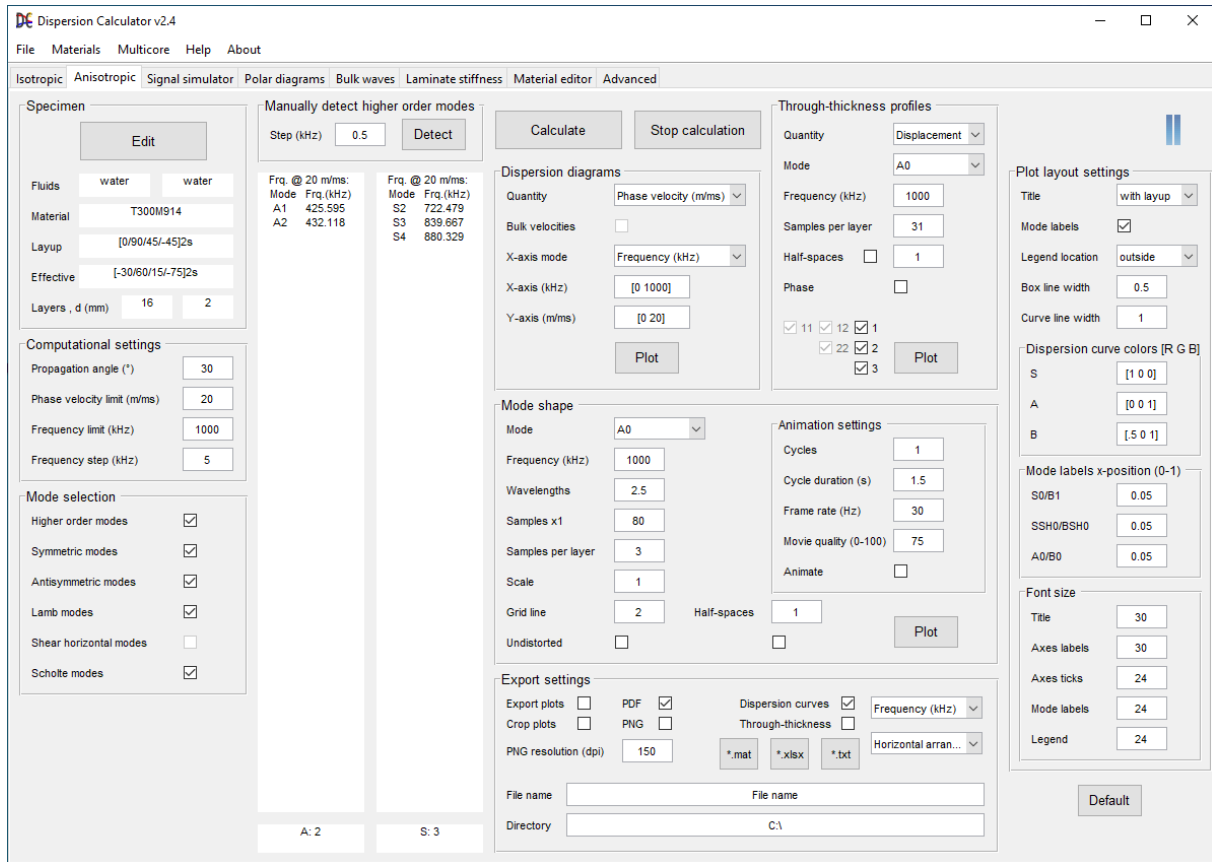


**Fig. 1** The screenshot shows the "Anisotropic" tab for the calculation of dispersion diagrams and mode shapes of guided waves in multilayered composites.

## 2.2 Functionality

DC has eight tabs, of which six cover the main tasks, one allows to enter material parameters, and the last one contains advanced options. The tabs are listed in Table 1.

**Table 1. Overview of the functionality in DC.**

| Tab | Functionality |
|---|---|
| **Isotropic** | Calculation of dispersion diagrams and mode shapes for isotropic plates (very fast computation by using the Rayleigh-Lamb equations) |
| **Anisotropic** | Calculation of dispersion diagrams and mode shapes for multilayered anisotropic laminates (using SMM) |
| **Signal simulator** | Simulation of the signal of single and multiple guided wave modes |
| **Polar diagrams** | Calculation of polar dispersion diagrams for multilayered anisotropic laminates |
| **Bulk waves** | Calculation of the bulk waves' phase and group velocities, slownesses, and polarization, propagating in anisotropic media as well as their scattering on solid-fluid interfaces |
| **Laminate stiffness** | Calculation of the homogenized stiffness tensor of laminates |
| **Material editor** | To enter engineering constants or stiffnesses of orthotropic, transversely isotropic, cubic, and isotropic materials as well as fluids |
| **Advanced** | Contains the advanced options for the dispersion curve tracing algorithm |

*2.2.1 Dispersion diagrams*

Clearly, the main purpose of DC is calculating dispersion diagrams for isotropic plates and multilayered anisotropic laminates, which may contain layers with different materials and material classes (orthotropic, transversely isotropic, cubic, and isotropic). In the "Isotropic" tab, only single isotropic layers can be considered, but the dispersion diagrams are calculated particularly fast through the implementation of the Rayleigh-Lamb equations. In the "Anisotropic" tab, SMM is used. Dispersion diagrams can be expressed as phase velocity, energy velocity, propagation time, coincidence angle, wavelength, wavenumber, and attenuation versus frequency or frequency-thickness product. DC plots the energy velocity instead of the group velocity because the latter is not valid in attenuated cases. In nonattenuated cases, energy and group velocity are equivalent. In anisotropic specimens for wave propagation in an off-principal direction, the energy velocity vector does not point in the wave propagation direction, i.e., it is not aligned with the wave vector. In this case, DC plots the energy velocity vector components along and normal to the propagation direction, the energy velocity vector magnitude and the skew angle between the energy velocity vector and the wave propagation direction. Inside the dispersion diagrams, as in all kinds of plots, one can click on a curve to display values. A tool is available to read values at constant frequency, phase velocity, wavelength, etc. One can export the plots to several formats, and the dispersion curve raw data can be exported to MATLAB®, Excel, and Txt files.
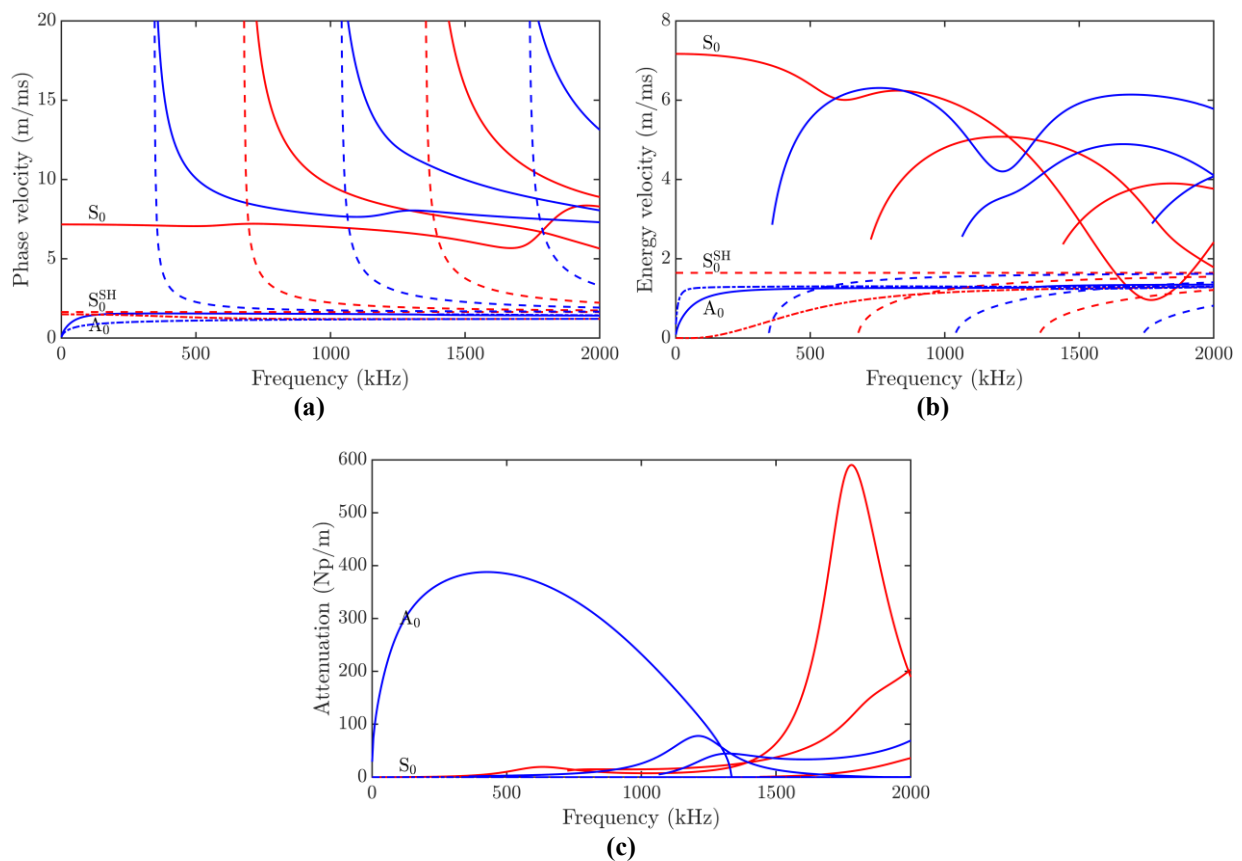


**Fig. 2** **Dispersion diagrams for wave propagation along 0° in a 2 mm thick [0/90]$_{4s}$ T800/913 composite immersed in water. (a) Phase velocity (b) energy velocity (c) attenuation.**

Fig. 2 shows dispersion diagrams for wave propagation along 0° in a 2 mm thick [0/90]$_{4s}$ T800/913 composite immersed in water. Lamb waves, indicated by solid lines, are decoupled

from SH modes, which are drawn as dashed lines. The Scholte modes propagating below the wave speed in water of 1500 m/s are drawn as dashed-dotted lines. As the laminate is symmetric, symmetric (red) and antisymmetric (blue) modes can be distinguished. Lamb waves are damped because energy radiates into the surrounding water. Therefore, they are often termed *leaky waves*. The amount of damping depends on the density ratio of the fluid with respect to the waveguide and on the out-of-plane displacement possessed by the various modes. As Fig. 2(c) shows, attenuation changes with frequency. $A_0$ with its predominant out-of-plane displacement at low frequencies is damped much stronger than $S_0$, which is dominated by in-plane displacement. Because SH waves are polarized exclusively in-plane (perpendicular to the propagation direction) and because the (inviscid) water does not support shear motion, SH waves do not couple to the water and therefore do not experience damping through energy leakage. The Scholte modes are not damped either because they propagate at or below the wave speed in the fluid. No material damping occurs in the considered waveguide because the material is assumed to be perfectly elastic.
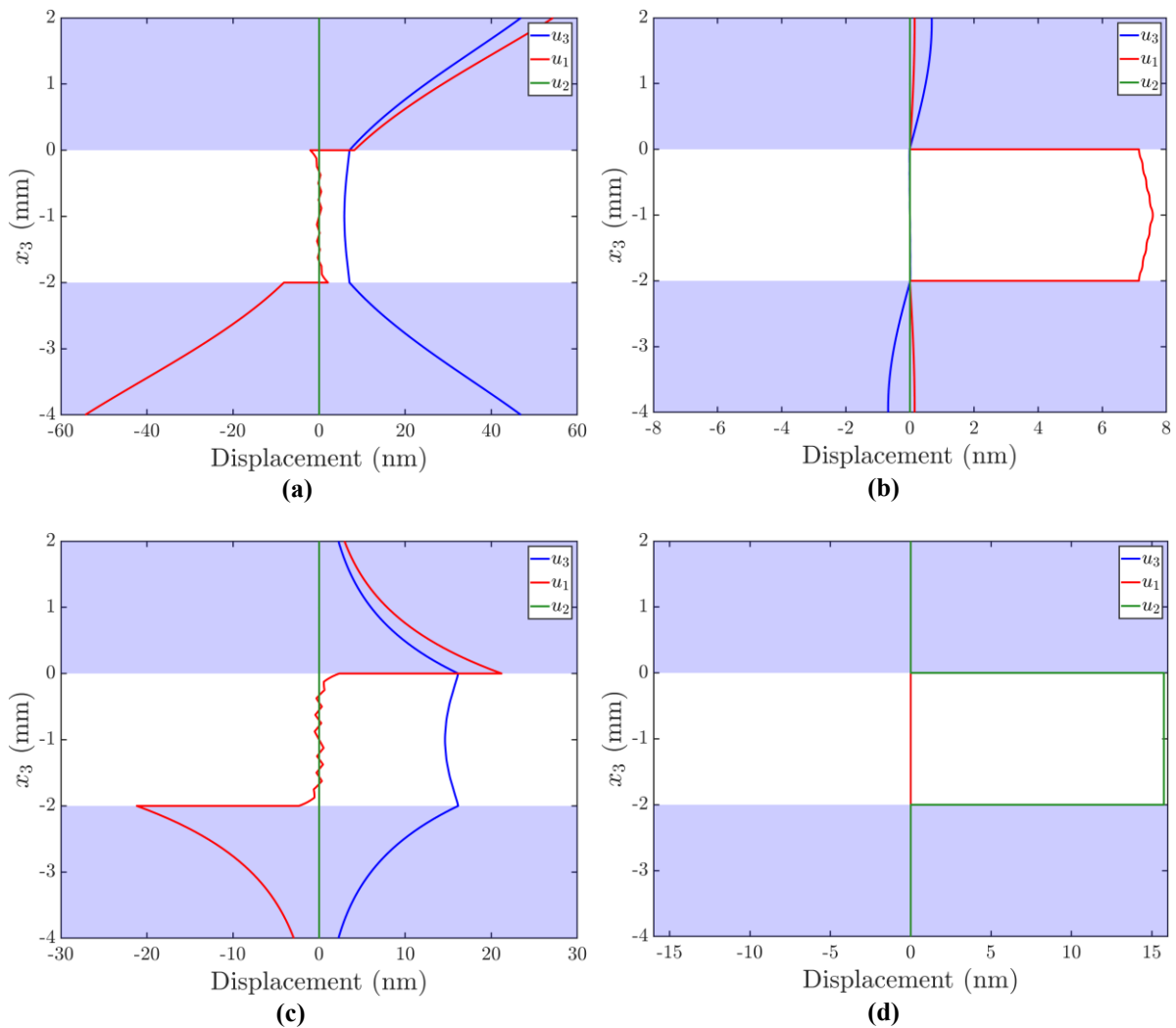


Fig. 3 Through-thickness displacement profiles at 200 kHz for wave propagation along 0° in a 2 mm thick [0/90]$_{4s}$ T800/913 composite immersed in water. (a) $A_0$ (b) $S_0$ (c) $A_0^{Scholte}$ (d) $S_0^{SH}$.

*2.2.2 Through thickness profiles and mode shapes*

For further investigation, one can select a mode and a frequency and plot the through-thickness displacement, stress, strain, energy density, and power flow density components. The profiles are helpful for finding out whether a mode is appropriate for detecting a certain type of flaw. The profiles are power-normalized similarly as in DISPERSE, i.e., the amplitudes are for guided waves carrying a power of 1 Watt in the propagation direction (neglecting the power flow in the fluid). All plots and the corresponding raw data can be exported.

Fig. 3(a) shows the displacement components of the $A_0$ Lamb wave at 200 kHz, based on the dispersion diagrams in Fig. 2. The composite is represented by the white area, while the upper and lower half-spaces are represented by the blue areas. The pure $A_0$ Lamb wave has nonzero out-of-plane and in-plane displacements $u_3$ and $u_1$, while the shear horizontal displacement $u_2$ is zero. Comparing Fig. 3(a) with $S_0$ at the same frequency in Fig. 3(b) illustrates how $A_0$ is vibrating predominantly in the out-of-plane direction whereas $S_0$ is dominated in-plane. Fig. 3(c) displays $A_0^{Scholte}$. In contrast to the leaky Lamb waves, which grow exponentially in the fluid-filled half-spaces (it can be seen more clearly when plotting the half-spaces farther away from the composite), $A_0^{Scholte}$ decays in the fluid. Although Scholte modes are interfaces waves in general, $A_0^{Scholte}$ in the present case would be useful for NDT because most displacement is confined inside the composite. Fig. 3(d) illustrates $S_0^{SH}$, possessing only nonzero shear horizontal displacement $u_2$ inside the composite and no interaction with the fluid.

A particularly useful representation for any researcher is the mode shape plot, such as that of $A_2$ displayed in Fig. 4. The mode shape plot gives a realistic view of how a certain mode at a certain frequency looks like. Notice in particular the wave fronts in the fluid and how the mode is damped with propagated distance. The mode shapes can be animated and movies or single frames can be exported.
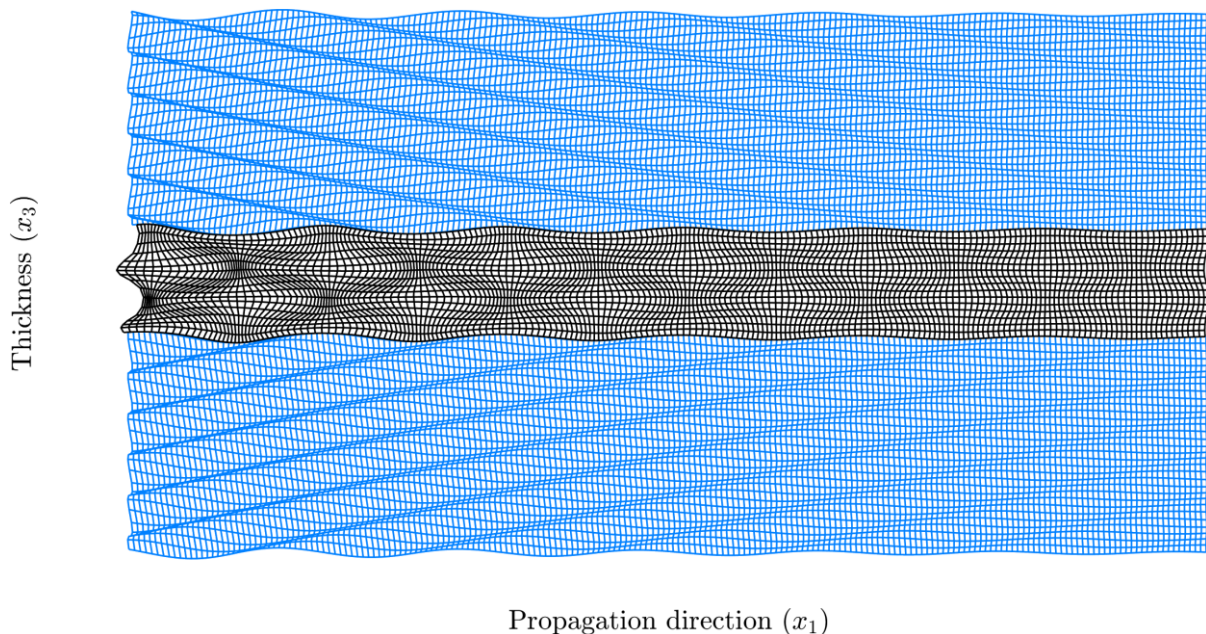


**Fig. 4**   **Mode shape of $A_2$ at 2000 kHz for wave propagation along 0° in a 2 mm thick [0/90]$_{4s}$ T800/913 composite immersed in water.**

### 2.2.3 Polar diagrams

Often it is useful to calculate polar diagrams for anisotropic specimens such as phase velocity, energy velocity, propagation time, coincidence angle, wavelength, and wavenumber versus propagation direction, respectively, ray angle, at a certain frequency. Basically, this is a top view on the composite, visualizing the behavior of guided wave propagation in anisotropic specimens. As usual, plots and raw data can be exported.

As an example, Fig. 5(a) displays the energy velocity vector magnitude $|\vec{c}_e|$ of the fundamental modes $A_0$, $S_0$, and $S_1$ at 200 kHz in a 1 mm thick layer T800/913 versus the ray angle $\Phi_r$. This kind of plot is also referred to as wavecrest plot. Basically, it shows how the guided waves generated by a point source advance outward with time. Therefore, these plots are useful for scenarios like acoustic emission where an array of sensors is placed on a specimen to detect ultrasonic signals emitted from a point source. By contrast, Fig. 5(b) plots the energy velocity component in the propagation direction $c_{e1}$ versus the propagation direction $\Phi$. This is useful, for example, when guided waves are excited and propagated in a certain direction $\Phi$ and captured with a sensor at some distance, as for example in air-coupled ultrasonic inspection. Suppose we excite a wave to propagate in the fiber direction (wave vector $\vec{k}$). The (phase) propagation direction $\Phi$ is 0° in this case. Because this is a principal direction, the wave packet, respectively, the acoustic beam, propagates at the same 0° direction. However, if we were to excite the wave, say, at 10° with respect to the fibers, the acoustic beam skews at some angle $\gamma$ towards the fibers because energy is transmitted more easily this way. Therefore, the acoustic beam propagates at the ray angle $\Phi_r$,

$$\Phi_r = \Phi - \gamma.$$

So, the energy velocity vector $\vec{c}_e$ points in $\Phi_r$, while the energy velocity component in the propagation direction $c_{e1}$ points in $\Phi$, i.e., along the wave vector $\vec{k}$. Because in an air-coupled ultrasonic inspection setup, the sensor is located at some distance in the propagation direction, we are interested in the energy velocity component $c_{e1}$ in this direction, not in $|\vec{c}_e|$. The skew angle versus propagation direction is plotted in Fig. 5(c). Accordingly, $\gamma$ is zero for wave propagation parallel and normal to the fibers ($\Phi = 0°$, 90°), i.e., $\Phi_r = \Phi$ and $c_e = c_{e1}$ ($c_{e2} = 0$). For example, the skew angle of $A_0$ for the phase propagation direction of 10° is 8.9° so that energy propagates at $\Phi_r = 1.1°$.

A few words should be said about the mode naming of $S_0$. This mode is often called $SH_0$ even in coupled cases in dispersion diagrams as well as in polar diagrams. However, this is physically incorrect and misleading as it implies that it is an SH mode with only shear horizontal displacement $u_2$, while $u_1$ and $u_3$ vanish. However, $S_0$ in Fig. 5 is polarized exclusively in the shear horizontal direction only for $\Phi = 0°$, 90°; for all other propagation directions, shear horizontal motion and sagittal plane motion are coupled. DC uses the term "SH" only in decoupled cases where pure Lamb and SH modes exist.
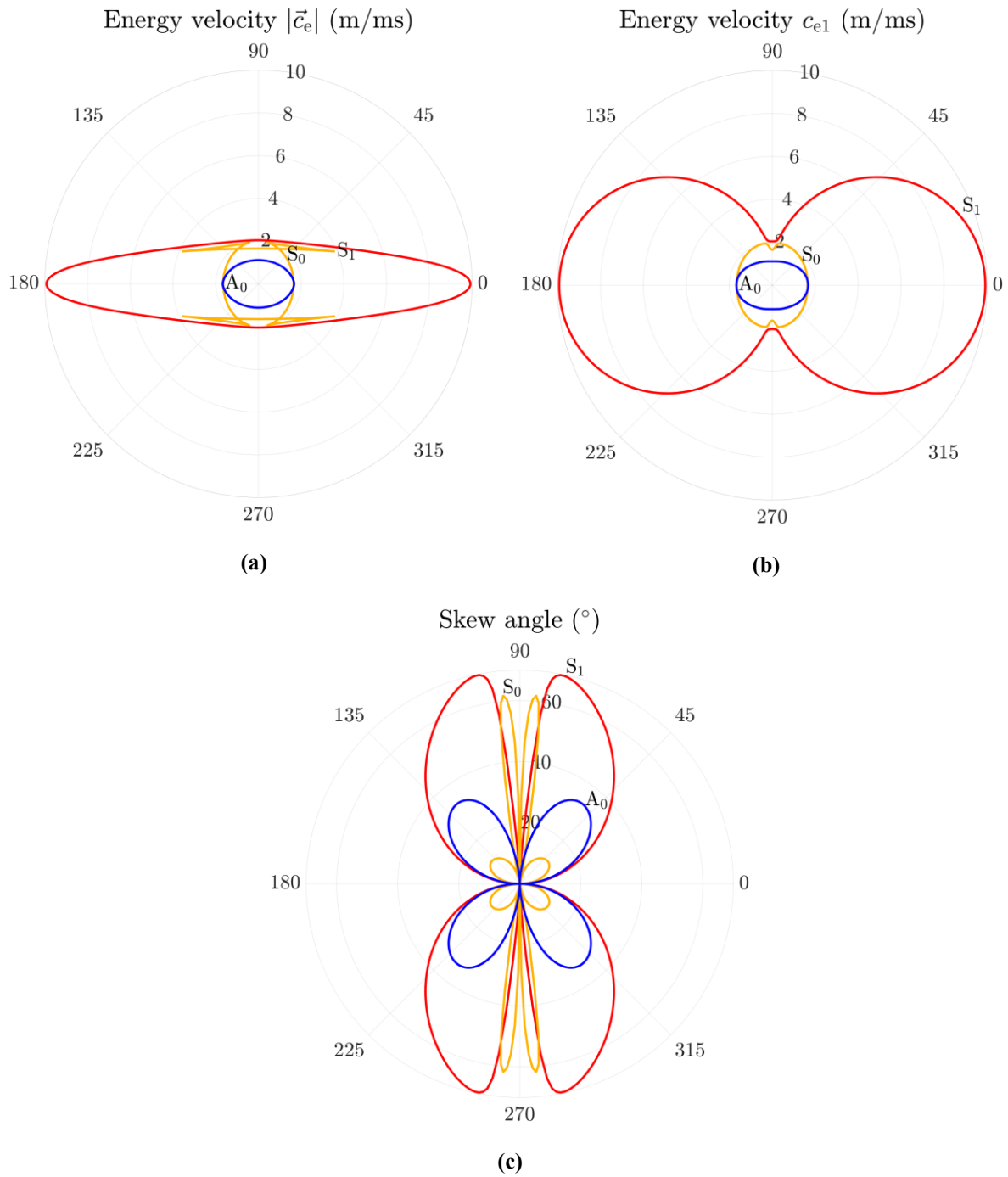
**Fig. 5    Polar energy velocity for the fundamental modes at 200 kHz in a 1 mm thick layer T800/913. (a) Energy velocity magnitude versus ray angle (b) energy velocity component in the propagation direction versus propagation direction (c) energy skew angle versus propagation direction.**

## *2.2.4 Signal simulator*

In any experimental setup involving guided waves, measured data are obtained as a signal of voltage versus time. The "Signal simulator" (see Fig. 6) predicts the temporal and frequency responses of single and multiple guided wave modes after propagating a certain distance in a specimen, based on the dispersion curves obtained in the "Isotropic" and "Anisotropic" tabs. Therefore, the tool is valuable to any individual performing NDI or SHM using guided waves. The dispersion diagrams calculated before help to excite the desired mode in a specimen. However, it is often difficult to excite only one particular mode, especially when the frequency-thickness product is large. In situations where dispersion curves are close to each other in the dispersion diagram, it is very likely that multiple modes are excited. Then, the inspector has to deal with multiple wave packets appearing in the measured signal. The Signal simulator helps identify the modes in the signal. The tool is also useful to interpret signals obtained from acoustic emission experiments. Or suppose we want to perform long-range testing on an aircraft wing structure. The dispersive nature of guided waves leads to a spreading and reduction in amplitude of the wave packet with increasing propagation distance because the different frequency components propagate at different phase velocities. Therefore, we would want to excite a weakly dispersive Lamb wave, retaining the shape of its wave packet over long distances. Another effect that becomes evident in the signals is damping due to fluid-loading and/or viscoelasticity. We would prefer a mode that suffers minimal damping loss in the required frequency range. With the Signal simulator, we can simulate the wave packets to find an appropriate mode for the task.
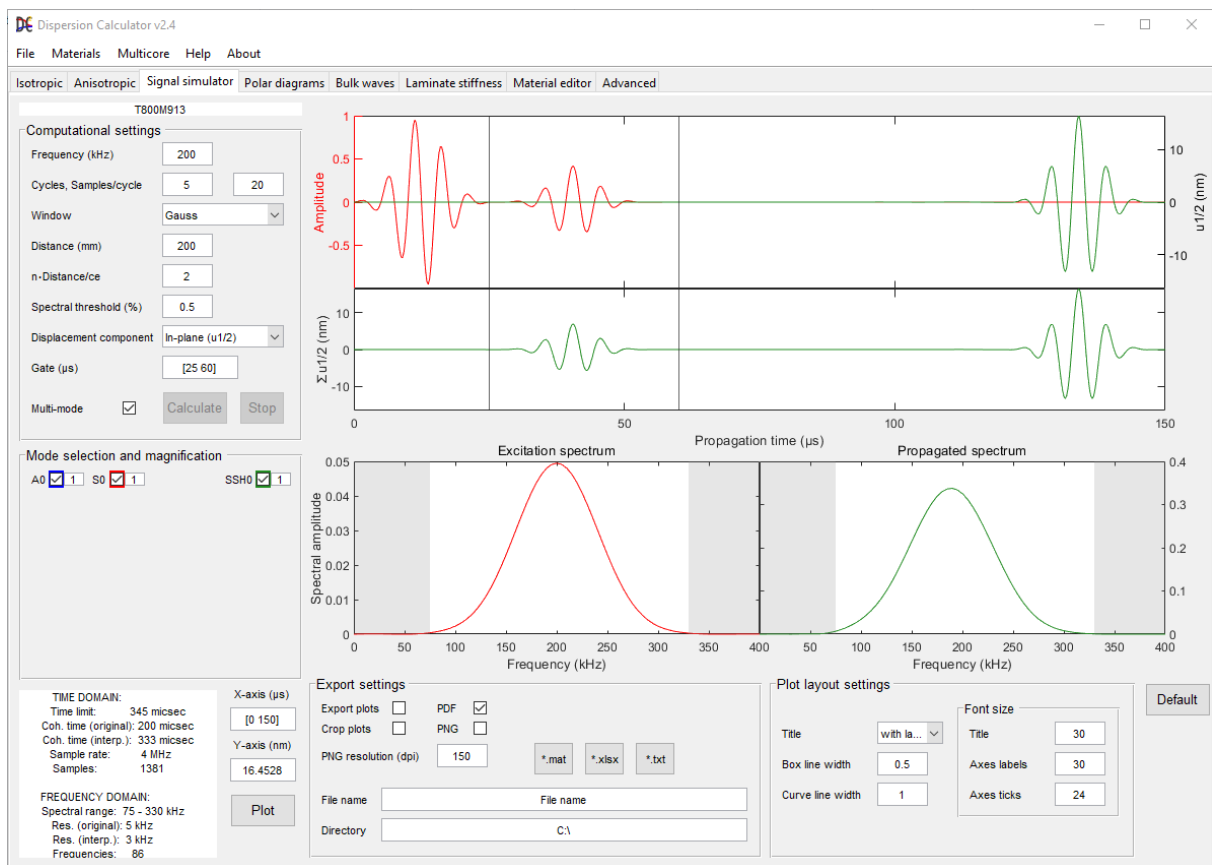


**Fig. 6    The "Signal simulator" predicts the temporal and frequency responses of guided waves after propagating a certain distance in a specimen.**

Notice that no particular method of excitation and reception is considered here. The assumption is that guided waves are generated *somehow* at $x = 0$, with the excitation signal plotted on the left-hand side in the upper signal window in Fig. 6, starting at $t = 0$. The propagated signal is calculated based on the dispersion diagrams obtained in the "Isotropic" or "Anisotropic" tabs. Plane harmonic waves are superposed, having the phase velocities and attenuations given by the dispersion curve of the respective mode in the frequency range seen in the excitation spectrum in Fig. 6. Power normalization is performed on each contributing plane wave in the same way as done in the through-thickness profiles. The plotted amplitude can be chosen as the out-of-plane displacement ($u_3$) for Lamb waves or the in-plane displacement ($u_1$) for Lamb waves and $u_2$ for SH waves. These displacements are calculated at the top of the plate where they are supposed to correlate most directly with the measured signal. The signal is simulated for ideal conditions, so experimentally measured signals will look more or less the same due to many influences present under real conditions. These are, for instance, the specific shape of the ultrasonic beam or a certain angle of incidence, whereas in the simulation, the "perfect" (coincidence) angle (for each contributing phase velocity in the spectrum) is assumed. Furthermore, waveguide imperfections are ignored such as surface roughness, layer debonding or other flaws. Calculating fully realistic signals requires a sophisticated model of the experimental setup, i.e., a detailed model of the sensors as well as of the waveguide to model the generated ultrasonic beam, the propagating wave field, and the received signal. This requires an FEM software such as COMSOL Multiphysics®. One can, however, choose to plot the in-plane or the out-of-plane displacement, depending on what component the considered sensor is more sensitive to. Usually, in noncontact air-coupled ultrasonics, one would choose the out-of-plane displacement, whereas in SHM where sensors are attached to the component, the in-plane displacement is more favored. In practice, the received signal maps a mixture of both components. The key point is that the Signal simulator calculates the displacement caused by the guided waves at the top surface, but the signal displayed on the measurement screen depends on how the sensor reacts to this displacement, and this is not included in the Signal simulator.

As an example, the signals of the fundamental modes $A_0$, $S_0$, and $S_0^{SH}$ after propagating a distance of 200 mm in the 0° direction in a $[0/90]_{4s}$ T800/913 composite immersed in water is simulated in Fig. 6, based on the dispersion curves in Fig. 2. A 5 cycles, 200 kHz sinusoidal carrier wave multiplied with a Gaussian window function is used to simulate the excitation wave packet drawn in red between $t = 0$ and 25 µs in the upper signal window. The excitation spectrum shows the spectral weights of the contributing frequencies, ranging from 75 to 330 kHz. The in-plane displacement is selected for the simulation. Two propagated wave packets appear in the upper signal window. The red one arriving at 28 µs is $S_0$, and the green one incoming at 120 µs is $S_0^{SH}$. $A_0$ is damped severely due to its strong coupling to the surrounding water. This tells us that we do not need to search for it in the measurement. $S_0^{SH}$ has the advantage of not coupling to the water at all so that it does not suffer damping, while $S_0$ diminishes with propagated distance. This makes $S_0^{SH}$ a good choice for long range testing in heavily fluid-loaded cases. Also, because $S_0^{SH}$ is nondispersive, the wave packet remains compact, whereas a dispersive mode's wave packet spreads, therefore loosing peak intensity and flaw localization resolution. The lower signal window shows the summation of all modes. In case of overlapping wave packets, it simulates the actual signal, while the upper window allows for identification of the contributions of the various modes. In the "Mode selection and magnification" panel, one can show or hide every mode and enter a magnification factor. Magnification is useful because the (displacement) amplitudes are calculated for a power flow of 1 Watt. However, in reality, each mode carries a different power flow because they are

excited and detected with different efficiency. Finally, extra plots can be generated and exported, and the raw data can be exported as well.

*2.2.5 Material editor*

Although DC has an extensive library of standard materials, it is necessary that the user can add custom material parameters. In the "Material editor" tab shown in Fig. 7, one can view the default materials and add or remove materials. For isotropic materials, one can either enter the engineering constants, or the stiffness components, or the bulk wave speeds. For anisotropic materials, one can enter only engineering constants or stiffness components. For convenience, the user can select the material symmetry class (orthotropic, transversely isotropic, or cubic). When selecting the transversely isotropic or cubic class only 5 or 3 of the 9 parameters remain active. Each parameter has a real part and an imaginary part. While the real part describes the harmonic wave propagation in the usual way, the imaginary part represents the damping. Therefore, only if all imaginary parts are zero, the material is perfectly elastic, i.e., without material damping. DC uses the hysteretic damping model, corresponding to a linear increase of attenuation with frequency, i.e., a constant loss per wavelength. For convenience, all viscoelastic default materials carry the suffix "viscoelastic". The material data can be exported and imported as txt-files via the "Materials" option in the menu bar. This is useful, for example, when the user wants to transfer custom materials to a new DC installation.
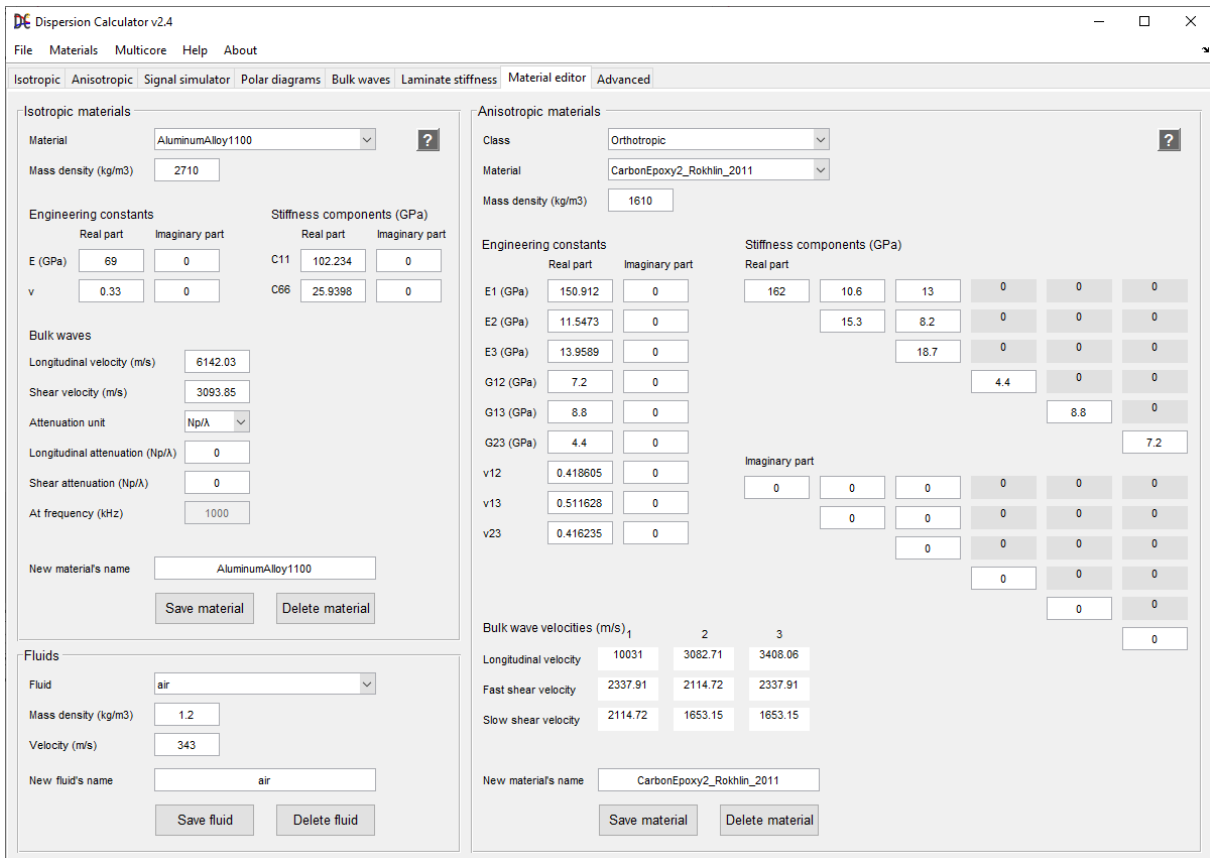


**Fig. 7** In the "Material editor", one can edit, add, or remove isotropic, cubic, transversely isotropic, and orthotropic materials as well as fluids.

## *2.3 Limitations and future work*

DC uses analytic dispersion equations, but such equations are available only for simple structures such as plates and cylinders. DC is currently limited to isotropic plates and multilayered anisotropic laminates such as composites, which can be viscoelastic and surrounded by fluids. However, dispersion curve computation for guided waves in isotropic rods and pipes including viscoelasticity and fluid-loading from inside and outside are on the way. Multilayered and anisotropic rods and pipes are scheduled later. There are no plans currently to implement a discretizing method such as SAFE or SCM to compute waveguides with arbitrary cross sections.

## *2.4 Download and installation*

DC is available on GitHub [28]. One can download the stand-alone installer, for which no MATLAB® is required, and one can download the MATLAB® code. When running the stand-alone installer, a MATLAB® runtime will be downloaded and installed automatically. In case the MATLAB® runtime is not downloaded and installed automatically, download it from https://www.mathworks.com/products/compiler/matlab-runtime.html and install it manually. The required runtime version number can be found in the change log file. For more information, see the README on GitHub [28].

## 3. Conclusions

In this paper, the open source DC, available at GitHub [28], was presented. DC is capable of calculating dispersion diagrams and mode shapes of guided waves in composite laminates containing several hundreds of layers, therefore enabling the modeling of guided waves in the thickest specimens like modern rocket booster pressure vessels. Damping induced through viscoelasticity and fluid-loading can be considered. DC is able to distinguish the different mode families like symmetric, antisymmetric, and nonsymmetric Lamb, SH and Scholte waves. DC features a highly efficient and robust dispersion curve tracing algorithm. An easy-to-use graphical user interface enables even a beginner to obtain results fast. DC was released initially in 2018 and has gained many users in the community since then.

## References

[1] I. Viktorov, "Rayleigh and Lamb Waves: Physical Theory and Applications," Plenum, New York, pp. 123-144 (1967)

[2] M. Luukkala, P. Heikkila, and J. Surakka, "Plate wave resonance - A contactless test method," Ultrasonics, Vol. 9, No. 4, pp. 201-208 (1971)

[3] M. Luukkala and P. Meriläinen, "Metal plate testing using airborne ultrasound," Ultrasonics, Vol. 11, No. 5, pp. 218-221 (1973)

[4] P. D. Wilcox, M. J. S. Lowe, and P. Cawley, "Mode and transducer selection for long range Lamb wave inspection," J. Intell. Mater. Syst. Struct., Vol. 12, pp. 553-565 (2001)

[5] M. J. S. Lowe, D. N. Alleyne, and P. Cawley, "Defect detection in pipes using guided waves," Ultrasonics, Vol. 36, pp. 147-154 (1998)

[6] M. J. S. Lowe and P. Cawley, "The applicability of plate wave techniques for the inspection of adhesive and diffusion bonded joints," J. Nondestr. Eval., Vol. 13, No. 4, pp. 185-200 (1994)

[7] T. Kundu, A. Maji, T. Gosh, and K. Maslov, "Detection of kissing bonds by Lamb waves," Ultrasonics, Vol. 35, pp. 573-580 (1998)

[8] K. Maslov and T. Kundu, "Selection of Lamb modes for detecting internal defects in composite laminates," Ultrasonics, Vol. 35, pp. 141-150 (1997)

[9] S. S. Kessler, S. M. Spearing, and C. Soutis, "Damage detection in composite materials using Lamb wave methods," Smart Mater. Struct., Vol. 11, pp. 269-278 (2002)

[10] N. Toyama, J. Noda, and T. Okabe, "Quantitative damage detection in cross-ply laminates using Lamb wave method," Compos. Sci. Technol., Vol. 63, pp. 1473-1479 (2003)

[11] Z. Su, L. Ye, and Y. Lu, "Guided Lamb waves for identification of damage in composite structures: A review," J. Sound Vib., Vol. 295, pp. 753-780 (2006)

[12] K. Diamanti and C. Soutis, "Structural health monitoring techniques for aircraft composite structures," Prog. Aeronaut. Sci., Vol. 46, pp. 342-352 (2010)

[13] A. S. Purekar and D. J. Pines, "Damage detection in thin composite laminates using piezoelectric phased sensor arrays and guided Lamb wave interrogation," J. Intell. Mater. Syst. Struct., Vol. 21, pp. 995-1010 (2010)

[14] C. Ramadas, K. Balasubramaniam, M. Joshi, and C. V. Krishnamurthy, "Sizing of interface delamination in a composite T-joint using time-offlight of Lamb waves," J. Intell. Mater. Syst. Struct., Vol. 22, pp. 757-768 (2011)

[15] H. Cunfu, L. Hongye, L. Zenghua, and W. Bin, "The propagation of coupled Lamb waves in multilayered arbitrary anisotropic composite laminates," J. Sound Vib., Vol. 332, pp. 7243-7256 (2013)

[16] A. Huber, "Non-destructive Testing of Future Rocket Boosters Using Air-Coupled Ultrasound", 19th World Conference on Non-Destructive Testing, pp. 1-9 (2016)

[17] M. Castaings and P. Cawley, "The generation, propagation, and detection of Lamb waves in plates using air-coupled ultrasonic transducers," J. Acoust. Soc. Am., Vol. 100, No. 5, pp. 3070-3077 (1996)

[18] M. Castaings, P. Cawley, R. Farlow, and G. Hayward, "Single sided inspection of composite materials using air coupled ultrasound," J. Nondestr. Eval., Vol 17, No. 1, pp. 37-45 (1998)

[19] M. Castaings and B. Hosten, "Lamb and SH waves generated and detected by air-coupled ultrasonic transducers in composite material plates," NDT&E Int., Vol. 34, pp. 249-258 (2001)

[20] M. Castaings and B. Hosten, "Ultrasonic guided waves for health monitoring of high-pressure composite tanks," NDT&E Int., Vol 41, pp. 648-655 (2008)

[21] I. Solodov, R. Stoessel, and G. Busse, "Material characterization and NDE using focused slanted transmission mode of air-coupled ultrasound," Res. Nondestr. Eval., Vol. 15, No. 2, 65-85 (2004)

[22] I. Solodov, K. Pfleiderer, H. Gerhard, and G. Busse, "Nonlinear acoustic approach to material characterisation of polymers and composites in tensile tests," Ultrasonics, Vol. 42, pp. 1011-1015 (2004)

[23] I. Solodov, K. Pfleiderer, H. Gerhard, S. Predak, and G. Busse, "New opportunities for NDE with air-coupled ultrasound," NDT&E Int., Vol. 39, No. 3, pp. 176-183 (2006)

[24] M. Rheinfurth, F. Schmidt, D. Döring, I. Solodov, G. Busse, and P. Horst, "Air-coupled guided waves combined with thermography for monitoring fatigue in biaxially loaded composite tubes," Compos. Sci. Technol., Vol. 71, No. 5, pp. 600-608 (2011)

[25] M. Rheinfurth, N. Kosmann, D. Sauer, G. Busse, and K. Schulte, "Lamb waves for non contact fatigue state evaluation of composites under various mechanical loading conditions," Composites: Part A, Vol. 43, pp. 1203-1211 (2012)

[26] B. Pavlakovic, M. J. S. Lowe, D. Alleyne, and P. Cawley, Rev. Prog. QNDE, "Disperse: A General Purpose Program for Creating Dispersion Curves," Plenum Press, New York, pp. 185-192 (1997)

[27] M. J. S. Lowe and B. Pavlakovic, "DISPERSE," http://www.imperial.ac.uk/non-destructive-evaluation/products-and-services/disperse

[28] A. Huber, "Dispersion Calculator," https://github.com/ArminHuber/Dispersion-Calculator

[29] P. Boccini, A. Marzani, and E. Viola, "Graphical User Interface for Guided Acoustic Waves," J. Comput. Civil. Eng., Vol. 25, pp. 202-210 (2011)

[30] A. Marzani and P. Bocchini, "GUIGUW v2.2.," http://www.guiguw.com

[31] D. R. Ramasawmy, B. T. Cox, and B. E. Treeby, "ElasticMatrix: A MATLAB toolbox for anisotropic elastic wave propagation in layered media," SoftwareX, Vol. 11, No. 100397, pp. 1-8 (2020)

[32] D. R. Ramasawmy, B. T. Cox, and B. E. Treeby, "Elastic matrix," https://github.com/dannyramasawmy/ElasticMatrix

[33] A. H. Orta, M. Kersemans, and K. V. D. Abeele, "A comparative study for calculating dispersion curves in viscoelastic multi-layered plates," Compos. Struct. Vol. 294, No. 115779 (2022)

[34] A. H. Orta, K. Van Den Abeele, and M. Kersemans, "The Dispersion Box," https://github.com/adilorta/The-Dispersion-Box

[35] D. A. Kiefer, "GEW dispersion script," https://doi.org/10.5281/zenodo.7010603

[36] Liu et al., "SAFEDC," https://sourceforge.net/projects/safedc

[37] S. I. Rokhlin and L. Wang, "Stable recursive algorithm for elastic wave propagation in layered anisotropic media: Stiffness matrix method," J. Acoust. Soc. Am., Vol. 112, No. 3, pp. 822-834 (2002)

[38] L. Wang and S. I. Rokhlin, "Stable reformulation of transfer matrix method for wave propagation in layered anisotropic media," Ultrasonics, Vol. 39, pp. 413-424 (2001)

[39] S. I. Rokhlin, D. E. Chimenti, and P. B. Nagy, "Physical Ultrasonics of Composites" Oxford University Press, Oxford (2011)

[40] V. G. A. Kamal and V. Giurgiutiu, "Stiffness transfer matrix method (STMM) for stable dispersion curves solution in anisotropic composites," Proc. SPIE, Vol. 9064 (2014)

[41] W. T. Thomson, "Transmission of elastic waves through as stratified solid medium," J. Appl. Phys., Vol. 21, pp. 89-93 (1950)

[42] N. A. Haskell, "The dispersion of surface waves on multilayered media," Bull. Seism. Soc. Am., Vol. 43, No. 1, pp. 17-34 (1953)

[43] A. H. Nayfeh, "The propagation of horizontally polarized shear waves in multilayered anisotropic media," J. Acoust. Soc. Am., Vol. 86, pp. 2007-2012 (1989)

[44] A. H. Nayfeh, "The general problem of elastic wave propagation in multilayered anisotropic media," J. Acoust. Soc. Am., Vol. 89, pp. 1521-1531, (1991)

[45] A. H. Nayfeh, "Wave Propagation in Layered Anisotropic Media with Applications to Composites", North-Holland, Amsterdam, pp. 1-152 (1995)

[46] L. Knopoff, "A matrix method for elastic wave problems," Bull. Seism. Soc. Am., Vol. 54, No. 1, pp. 431-438 (1964)

[47] H. Schmidt and G. Tango, "Efficient global matrix approach to the computation of synthetic seismograms," Geophys. J. R. Astr. Soc., Vol. pp. 84, 331-359 (1986)

[48] A. K. Mal, "Wave propagation in layered composite laminates under periodic surface loads," Wave Motion, Vol. 10, No. 3, pp. 257-266 (1988)

[49]  E. Kausel and J. M. Roesset, "Stiffness matrices for layered soils," Bull. Seis. Soc. Am., Vol. 71, No. 6, pp. 1743-1761 (1981)

[50]  M. J. S. Lowe, "Matrix Techniques for Modeling Ultrasonic Waves in Multilayered Media," IEEE Trans. Ultrason. Ferroelec. Freq. Contr., Vol. 42, pp. 525-542 (1995)

[51]  A. M. A. Huber and M. G. R. Sause, "Classification of solutions for guided waves in anisotropic composites with large numbers of layers," J. Acoust. Soc. Am., Vol. 144, pp. 3236-3251 (2018)

[52]  A. M. A. Huber, "Classification of solutions for guided waves in fluid-loaded viscoelastic composites with large numbers of layers," J. Acoust. Soc. Am., Vol. 154, pp. 1073-1094 (2023)

[53]  A. Huber, "Numerical modeling of guided waves in anisotropic composites with application to air-coupled ultrasonic inspection," https://elib.dlr.de/139819 (2020)

[54]  L. Gavric, "Computation and propagative waves in free rail using a finite element technique," J. Sound Vib., Vol. 185, No. 3, pp. 531-543 (1995)

[55]  F. H. Quintanilla, M. J. S. Lowe, and R. V. Craster, "Modeling guided elastic waves in generally anisotropic media using a spectral collocation method," J. Acoust. Soc. Am., Vol. 137, No. 3, pp. 1180-1194 (2015)

[56]  F. H. Quintanilla, M. J. S. Lowe, and R. V. Craster, "The symmetry and coupling properties of solutions in general anisotropic multilayer waveguides," J. Acoust. Soc. Am., Vol. 141, No. 1, pp. 406-418 (2017)

[57]  D. Kiefer, M. Ponschab, S. Rupitsch, and M. Mayle, "Calculating the full leaky Lamb wave spectrum with exact fluid interaction," J. Acoust. Soc. Am., Vol. 145, No. 6, pp. 3341-3350 (2019)

[58]  E. Georgiades, M. Lowe, and R. Craster, "Leaky wave characterisation using spectral methods," J. Acoust. Soc. Am. Vol. 152, No. 3, pp. 1487-1497 (2022)

[59]  R. D. Mindlin, "Influence of rotatory inertia and shear flexural motions of isotropic elastic plates," J. Appl. Mech., Vol. 18, No. 1, pp. 31-38 (1951)

[60]  J. Whitney and C. Sun, "A higher order theory for extensional motion of laminated composites," J. Sound Vib., Vol. 30, No. 1, 85-97 (1973)

[61]  L. Wang and F. Yuan, "Lamb wave propagation in composite laminates using a higher-order plate theory," in: Nondestructive Characterization for Composite Materials, Aerospace Engineering, Civil Infrastructure, and Homeland Security 2007, Vol. 65310I (2007)

[62]  J. Zhao, H. Ji, and J. Qiu, "Modeling of Lamb waves in composites using new third-order plate theories," Smart Mat. Struct., Vol. 23, No. 4 (2014)

[63]  A. Han Orta, J. Vandendriessche, M. Kersemans, W. Van Paepegem, N. B. Roozen, K. Van Den Abeele, "Modeling lamb wave propagation in visco-elastic composite plates using a fifth-order plate theory," Ultrasonics, Vol. 116 (2021)